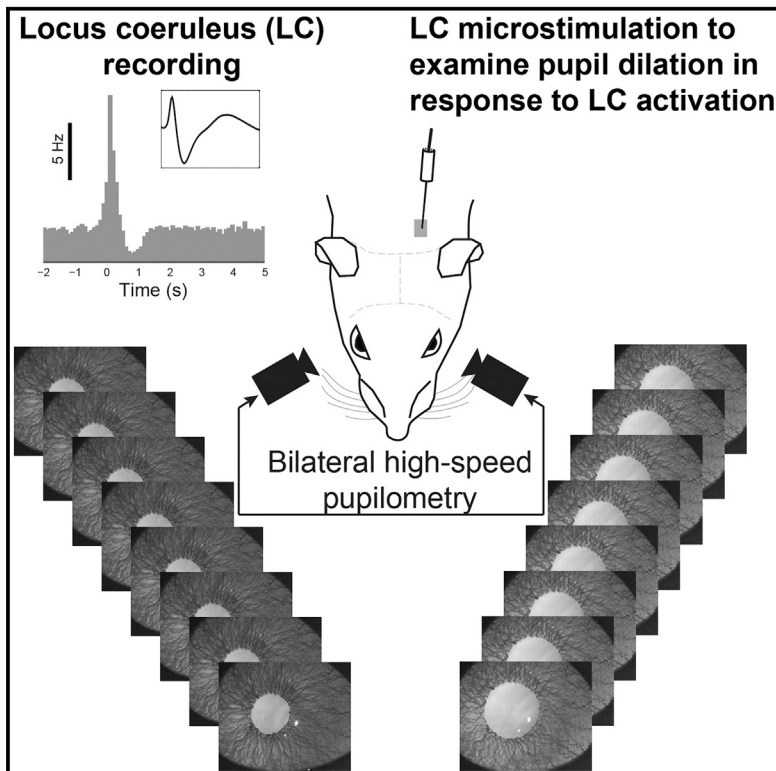


Dynamic Lateralization of Pupil Dilation Evoked by Locus Coeruleus Activation Results from Sympathetic, Not Parasympathetic, Contributions

Graphical Abstract



Authors

Yang Liu, Charles Rodenkirch, Nicole Moskowitz, Brian Schriver, Qi Wang

Correspondence

qi.wang@columbia.edu

In Brief

Liu et al. show that unilateral LC activation evokes bilateral but lateralized pupil dilation. This lateralization is dependent on the frequency of LC activation, which results from sympathetic, but not parasympathetic, contributions. This suggests a non-invasive technique for indexing autonomic imbalances in disorders involving the autonomic nervous system.

Highlights

- Unilateral LC activation evokes lateralized, bilateral pupil dilation
- Lateralization is dependent on the frequency of LC activation
- Dynamic lateralization arises from sympathetic, not parasympathetic, contributions
- Across-eye differences in dilation may provide a possible index of sympathetic tone



Dynamic Lateralization of Pupil Dilation Evoked by Locus Coeruleus Activation Results from Sympathetic, Not Parasympathetic, Contributions

Yang Liu,¹ Charles Rodenkirch,¹ Nicole Moskowitz,¹ Brian Schriver,¹ and Qi Wang^{1,2,*}

¹Department of Biomedical Engineering, Columbia University, New York, NY 10027, USA

²Lead Contact

*Correspondence: qi.wang@columbia.edu

<http://dx.doi.org/10.1016/j.celrep.2017.08.094>

SUMMARY

Pupil size is collectively controlled by the sympathetic dilator and parasympathetic sphincter muscles. Locus coeruleus (LC) activation has been shown to evoke pupil dilation, but how the sympathetic and parasympathetic pathways contribute to this dilation remains unknown. We examined pupil dilation elicited by LC activation in lightly anesthetized rats. Unilateral LC activation evoked bilateral but lateralized pupil dilation; i.e., the ipsilateral dilation was significantly larger than the contralateral dilation. Surgically blocking the ipsilateral, but not contralateral, sympathetic pathway significantly reduced lateralization, suggesting that lateralization is mainly due to sympathetic contribution. Moreover, we found that sympathetic, but not parasympathetic, contribution is correlated with LC activation frequency. Together, our results unveil the frequency-dependent contributions of the sympathetic and parasympathetic pathways to LC activation-evoked pupil dilation and suggest that lateralization in task-evoked pupil dilations may be used as a biomarker for autonomic tone.

INTRODUCTION

Mounting experimental data from humans, non-human primates, and rodents show that nonluminance-induced changes in pupil size are tightly correlated with arousal and various cognitive factors (Ebitz et al., 2014; Eldar et al., 2013; Hong et al., 2014; McCormick et al., 2015; McGinley et al., 2015a; Nassar et al., 2012; Reimer et al., 2014; Vinck et al., 2015). Recent work demonstrated a consistent difference in pupil dilation across two eyes in an attentional task and suggested that the level of this lateralization was collectively modulated by the attentional load and arousal (Wahn et al., 2017). Activity of the locus coeruleus (LC) has also been related to arousal and cognitive processing (Clayton et al., 2004; Nassar et al., 2012; Sara and Bouret, 2012; Sara et al., 1994), leading many to hypothesize that the LC mediates the dilations seen during cognitive processing (Aston-Jones and Cohen, 2005). The LC is also the primary source

of norepinephrine (NE) to the forebrain (Aston-Jones and Cohen, 2005; Berridge and Waterhouse, 2003; Sara, 2009; Szabadi, 2013). NE release results in a spectrum of modulatory effects on neural representation and computations through its action on adrenergic receptors (Ego-Stengel et al., 2002; Hirata et al., 2006; Martins and Froemke, 2015; McCormick and Pape, 1990; McGinley et al., 2015b; Moxon et al., 2007; Wekselblatt and Niell, 2015). The LC fires in two modes: tonic (i.e., long-term, continuous spiking at a rate of 1–5 Hz) and phasic, which manifests as sparsely occurring, transient, bursting events (Aston-Jones and Cohen, 2005). These modes are thought to have important behavioral relevance (Aston-Jones et al., 1994, 1996; Bouret and Richmond, 2015; Clayton et al., 2004; Kalwani et al., 2014; Rajkowski et al., 2004; Usher et al., 1999) and are hypothesized to separately affect pupil size, with tonic and phasic activation influencing baseline pupil size and transient pupil dilations, respectively; both of these were shown to reflect different cognitive factors (de Gee et al., 2014; Nassar et al., 2012).

Pupil size is determined by a balancing act between two smooth muscles: the sphincter and dilator pupillae muscles of the iris (Andreassi, 2006). The dilator muscle is innervated by sympathetic neurons in the superior cervical ganglion (SCG), which is, in turn, innervated by the intermediolateral cell column (IML) of the spinal cord. The sphincter muscle is innervated by parasympathetic neurons in the ciliary ganglion (CG), which is, in turn, innervated by the Edinger-Westphal nucleus (EWN). Thus, either excitation of the sympathetic SCG neurons or inhibition of the parasympathetic EWN neurons results in pupil dilation. Recent work established a causal link between LC activation and pupil size by showing that a brief phasic electrical microstimulation of the LC elicited transient dilation, when measured unilaterally, in monkeys and rodents (Joshi et al., 2016; Reimer et al., 2016). However, little is known about the dynamics of bilateral pupil dilation in response to different modes of LC activation. In addition, the functional contributions of the sympathetic and parasympathetic systems to LC activation-evoked dilations remain unclear.

Here we investigated the pupil dilations elicited by tonic and phasic activation of the LC in lightly isoflurane-anesthetized rats and present several findings that substantially elucidate the neural circuitry mediating the relationship between LC activation and pupil size. We show that unilateral LC activation evoked dilations for both pupils. Furthermore, the dilations were lateralized (i.e., ipsilateral dilation was significantly larger

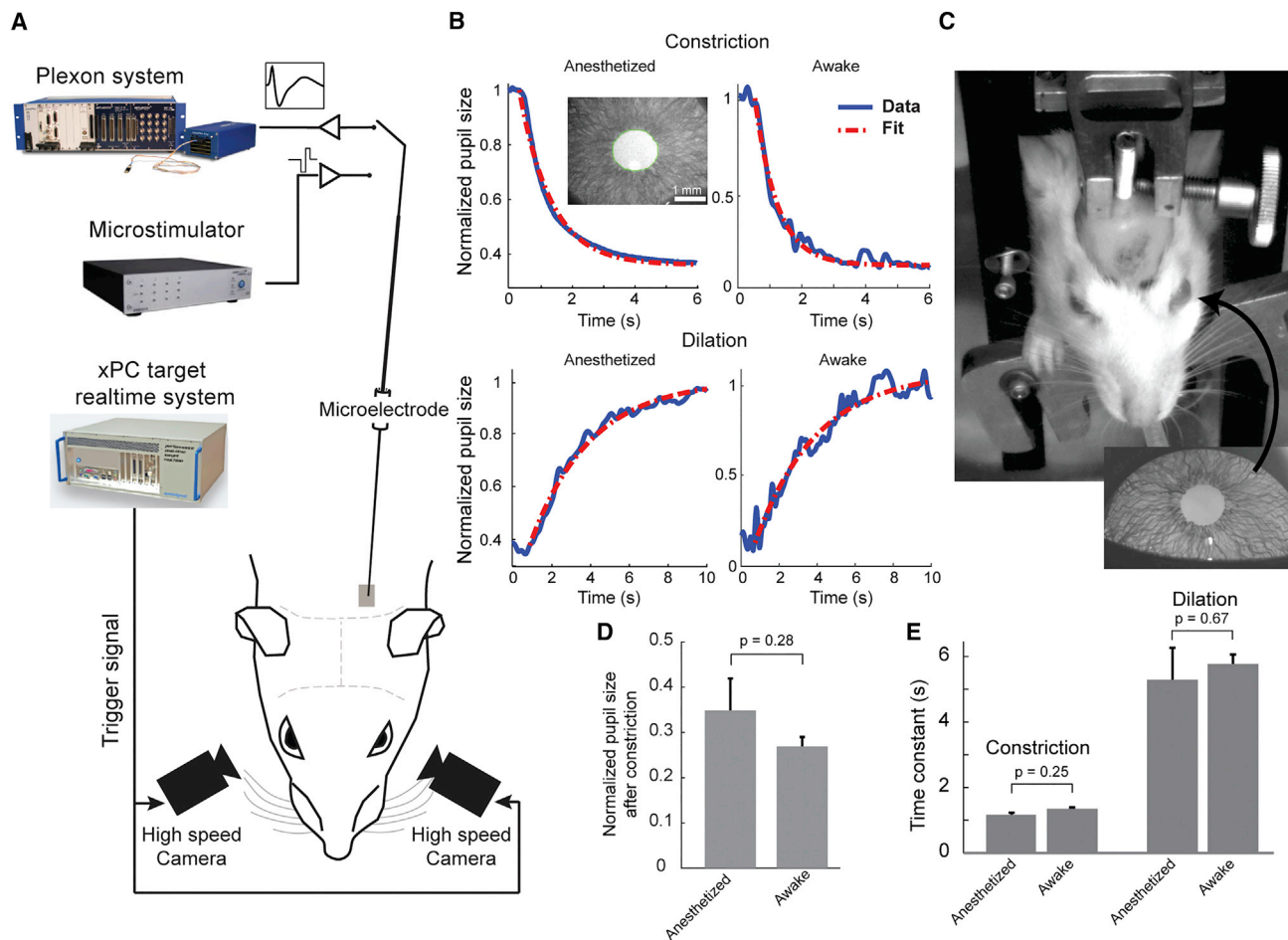


Figure 1. Pupillometry and Pupillary Light Reflex in Both Lightly Isoflurane-Anesthetized and Awake Rats

(A) Experimental setup to measure bilateral pupil response to LC activation. Both pupils in lightly anesthetized rats were imaged during electrical microstimulation of the LC. Single-unit extracellular recordings of the LC were obtained prior to stimulation to ensure correct microelectrode placement.

(B) Example pupillary light reflex (PLR) in anesthetized and awake animals. Top: pupil constriction following ambient lighting being switched from 15 to 150 lux. Bottom: pupil dilation following ambient lighting being switched from 150 to 15 lux. Inset: example pupil image with the green circle depicting automatically segmented pupil contour.

(C) An awake, head-constrained rat during PLR measurement and a close-up view of the easily segmented, reflective pupil.

(D) Normalized constriction amplitude of PLR for anesthetized and awake animals.

(E) The time constants of PLR in lightly anesthetized rats are not significantly different from those in awake rats.

Error bars indicate SEM.

than contralateral dilation), and tonic LC stimulation resulted in more lateralization than phasic LC stimulation, indicating that the difference between the dilations of the two pupils depends on the frequency of LC activation. Next, by pharmacologically and surgically blocking the EWN and SCG, we demonstrated that LC control of pupil size must only involve the parasympathetic EWN and sympathetic SCG, respectively. Finally, through removal of either the ipsilateral or contralateral SCG—i.e., superior cervical ganglionectomy (SCGx)—we found that the LC influenced the ipsilateral pupil through both parasympathetic and sympathetic pathways but influenced the contralateral pupil only through the parasympathetic pathway. Therefore, differences between bilateral pupil dilations were attributed to sympathetic contribution, suggesting these differences as a possible index for autonomic tone.

RESULTS

Pupil Dilation in Response to Phasic LC Activation and Pupillary Light Reflex Does Not Significantly Differ between Lightly Isoflurane-Anesthetized Rats and Awake Rats

All pupillometry data showing responses to tonic or phasic LC stimulation were recorded from rats lightly anesthetized with isoflurane (approximately 1% during recording) (Figure 1A). Because pupil dilation and constriction are mediated by the dilator and sphincter muscles, respectively (Lowenstein and Loewenfeld, 1962), we first tested whether isoflurane anesthesia significantly altered the response properties of these muscles by comparing the pupillary light reflex properties of the lightly isoflurane-anesthetized rats (Figure 1B; $n = 4$) with

those of awake rats (Figure 1C; $n = 3$). For both anesthetized and awake animals, switching ambient luminance from 15 to 150 lux resulted in rapid pupil constriction (with the pupil constricting to $35.5\% \pm 5.8\%$ of the baseline for the anesthetized animals and $26.9\% \pm 1.5\%$ for the awake animals, $p = 0.28$, Mann-Whitney U test, mean \pm SEM; Figure 1D), with the pupil gradually relaxing back to the baseline when the ambient luminance was switched back to 15 lux (Figure 1B). Changes in pupil size were fit with exponential decay or growth curves, respectively (Figure 1B). Time constants of the curves fit to pupil contraction and dilation were not significantly different between anesthetized and awake rats (Figure 1E; constriction: 1.135 ± 0.094 s versus 1.32 ± 0.098 s, $p = 0.248$, Mann-Whitney U test; dilation: 5.25 ± 1.01 s versus 5.74 ± 0.41 s, $p = 0.668$, Mann-Whitney U test; mean \pm SEM). To further test whether LC-mediated pupil dilation is affected by anesthesia, we measured pupil dilation evoked by 50 Hz phasic LC stimulation in three awake, head-constrained animals (Figure S1A). In our awake animals, although the ambient illuminance was constant during each session, and there was no behavioral task involved, pupil size tended to fluctuate both across and within trials (Joshi et al., 2016). LC stimulation with an amplitude of 60 or 100 μ A failed to elicit a distinguishable pupil dilation from background fluctuation for the animals, presumably because of scar tissue formation around the implanted electrodes (Ersen et al., 2015). Thus, we used an amplitude of 150 μ A for these awake animals (Experimental Procedures). LC phasic stimulation with this amplitude evoked dilation for both pupils ($37.3\% \pm 6.1\%$ for the ipsilateral pupil and $31.6\% \pm 5.5\%$ for the contralateral pupil, mean \pm SEM; Figure S1B). The time course of the dilations was not significantly different between the anesthetized and awake animals (ipsilateral rising stage: 1.38 ± 0.16 s versus 1.47 ± 0.10 s, $p = 0.76$; contralateral rising stage: 1.38 ± 0.18 s versus 1.22 ± 0.23 s, $p = 0.57$; ipsilateral decaying stage: 4.66 ± 0.89 s versus 4.48 ± 2.17 s, $p = 0.93$; contralateral decaying stage: 4.84 ± 0.61 versus 4.06 ± 1.1 s, $p = 0.52$; Mann-Whitney U test; Figure S1C). Importantly, the lateralization ratio was similar between the anesthetized and awake animals (1.25 ± 0.038 versus 1.21 ± 0.085 , $p = 0.62$, Mann-Whitney U test; Figure S1D). Therefore, these results suggest that light isoflurane anesthesia does not significantly disrupt LC mediated changes in pupil size and that the pupil size changes in response to LC stimulation presented in this study approximate the dynamic changes seen in awake animals.

Electrophysiology: Identification of LC Neurons

Single-unit recordings of LC cells were obtained using sharp tungsten microelectrodes with an impedance of approximately 2 M Ω (Figure 2A). LC cells were reliably found 5.5–6.2 mm below the brain surface. All recordings contained either a single large-amplitude unit or two units that could be isolated without ambiguity using principal-component analysis (PCA) sorting techniques. Expected anatomical location and electrophysiological characteristics of LC neurons, including a low spontaneous firing rate, wide waveform (>1.8 ms), and phasic response to paw pinch, were used to confirm microelectrode placement within the LC (Aston-Jones et al., 1991; Vazey and Aston-Jones, 2014). For all experiments, electrode placement

in the LC was further confirmed with post-experiment histological analysis (Figure 2B; Experimental Procedures). In response to a paw/tail pinch, LC cells typically fire a brief burst of 3–6 spikes with short interspike intervals (ISIs), which is usually followed by sustained suppression (>500 ms) of firing activity (Aston-Jones and Bloom, 1981; Clayton et al., 2004; Devilbiss and Waterhouse, 2011; Kalwani et al., 2014). The mean firing rate during the suppression period (500–1,000 ms after the paw/tail pinch) was significantly lower than both the baseline firing rate and mean firing rate within the 500 ms immediately following the paw/tail pinch (Figures 2C and 2D; $p < 0.001$, paired Wilcoxon signed-rank test). A paw pinch also evoked pupil dilation. Although the paw pinch-evoked pupil dilation may engage other brain structures besides the LC (Chapman et al., 1999), pupil dilation in response to the paw pinch exhibited a lateralization with a ratio of 1.68 ± 0.23 ($n = 2$; Figures S2A and S2B), suggesting that lateralized pupil dilation is a general phenomenon. We also found no significant correlation between the changes in pupil size and LC activity in response to paw pinch ($n = 2$, $p > 0.25$). However, this lack of significance could be due to the involvement of other circuitry (Chapman et al., 1999) or the small sample size. Future work is necessary to further examine this.

The mean firing rate, during the period of 500 ms following the paw/tail pinch, when phasic firing is present, was approximately 7 Hz. However, the ISIs of single-unit activity during this time period were widely distributed, ranging from several milliseconds to a couple hundreds of milliseconds. The peak of the ISI distribution was at approximately 40 ms, but a small number of spikes had ISIs shorter than 20 ms (Figure 2E; Figure S2C). We also observed single unit spikes with ISIs as short as ~ 3 ms during phasic responses (Figure 2F). Although the evoked firing of neurons next to a stimulating electrode is dependent on many factors, including electrode properties and relative position (Ranck, 1975), when attempting to phasically activate the LC through microstimulation, we used stimulation patterns with an inter-stimulus interval of both 20 ($n = 10$) and 3 ms ($n = 32$), which, we found, allowed us to examine the extent to which the frequency of LC activation affects the contribution of the sympathetic and parasympathetic pathway.

LC Stimulation Desynchronizes the Cortical EEG

We first examined whether activation of LC-NE neurons using electrical microstimulation would alter cortical arousal by shifting the power spectrum of the cortical electroencephalogram (EEG), as has been shown previously using pharmacological compounds (Berridge and Foote, 1991; Steriade et al., 1993; Vazey and Aston-Jones, 2014) and photostimulation (Li et al., 2016). Consistent with previous work, brief electrical microstimulation (50 Hz, 6 biphasic current pulses, 200 μ s per phase, 60- or 120- μ A amplitude) of the LC induced the EEG power spectrum to shift toward higher frequencies (Figure 3A), quantifiable by an increase in the ratio of 10–100 Hz to 1–10 Hz power ($p < 0.02$, Wilcoxon signed-rank test; Figure 3B). 60- μ A LC stimulation caused less desynchronization than 120- μ A LC stimulation (Figure 3B), suggesting that the observed desynchronization of the cortical EEG was due to activation of the LC.

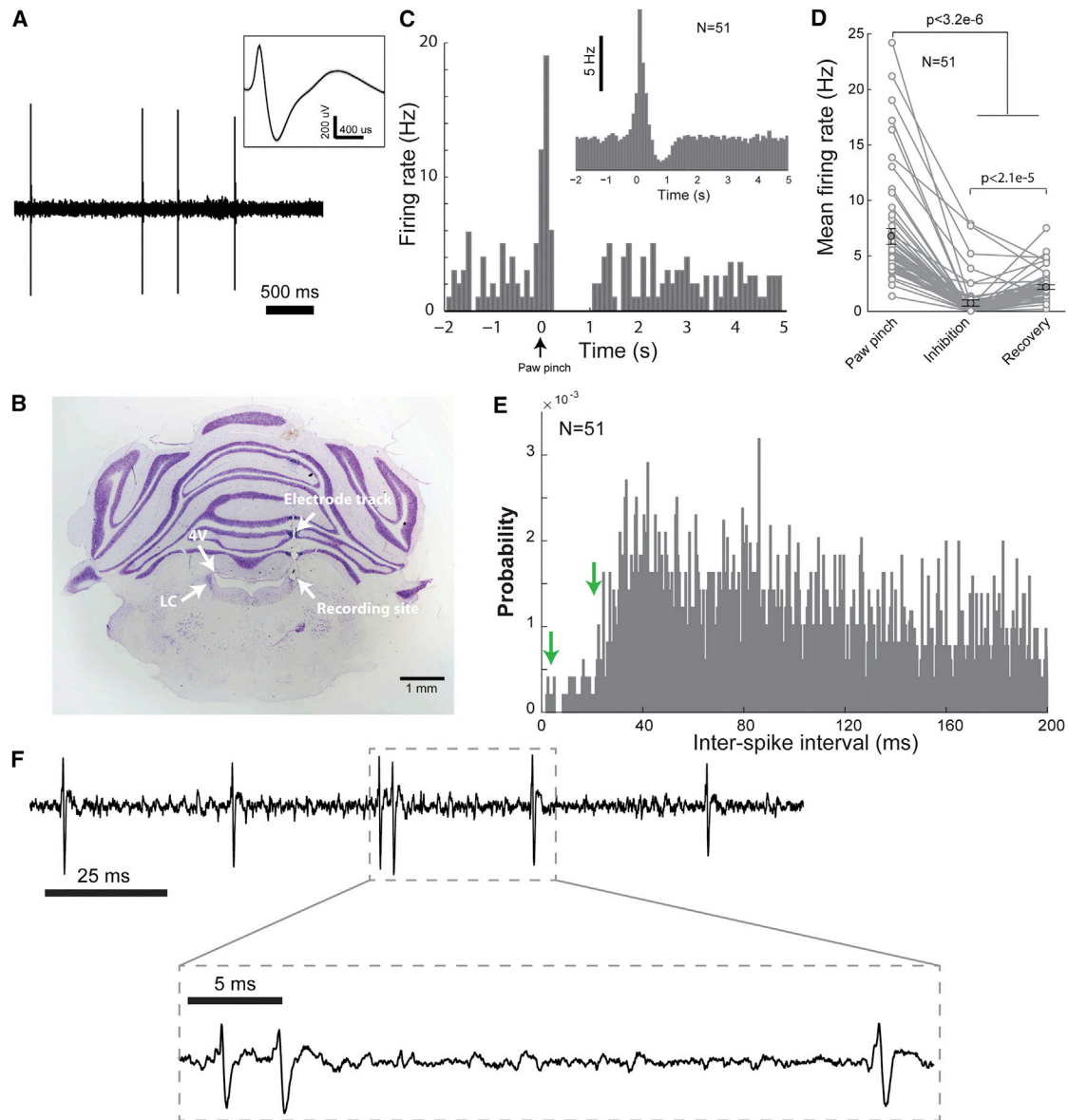


Figure 2. Electrophysiology of LC Neurons

(A) Example single-unit recording of spontaneous LC activity. Inset: typical wide waveform of LC neurons.

(B) A Nissl-stained brain slice, confirming correct placement of the microelectrode in the LC.

(C) A single-unit example of the characteristic phasic firing of LC neurons in response to a paw pinch (bin size, 100 ms). Time zero indicates the time of the paw pinch. Inset: the population peristimulus time histogram (PSTH) before and after the tail/paw pinch for 51 different LC neurons.

(D) Mean firing rate of the same 51 LC neurons during the 500 ms following the tail/paw pinch, the following suppression period, and, finally, the recovery period.

(E) The distribution of inter-spoke intervals for all phasic LC responses to the tail/paw pinch, binned at 0.5 ms. The arrows on the plot indicate the inter-spoke intervals our phasic microstimulation patterns were designed to mimic (left arrow, 3 ms [i.e., 333 Hz]; right arrow, 20 ms [i.e., 50 Hz]). Bin width, 0.5 ms.

(F) Example phasic LC activity containing spikes with an ISI of approximately 3 ms.

Error bars indicate SEM.

Tonic and Phasic LC Stimulation Elicits Bilateral Pupil Dilation with Different Temporal Characteristics

Phasic LC stimulation (6 biphasic pulses, 200 μ s per phase, 60 μ A, 3-ms or 20-ms inter-pulse interval; [Experimental Procedures](#)) was delivered following tonic LC stimulation (biphasic pulses with either 0, 0.5, 1, 2, or 5 Hz for 10 s, 200 μ s per phase,

60 μ A) meant to mimic the natural tonic firing patterns of the LC. Pupil dilation was measured as the change in pupil size following LC stimulation divided by the pupil size in a resting state. Both tonic and phasic unilateral LC microstimulation ($n = 15$ for the left LC, $n = 2$ for right LC) elicited pupil dilation for both the ipsilateral and contralateral eyes. The temporal characteristics of

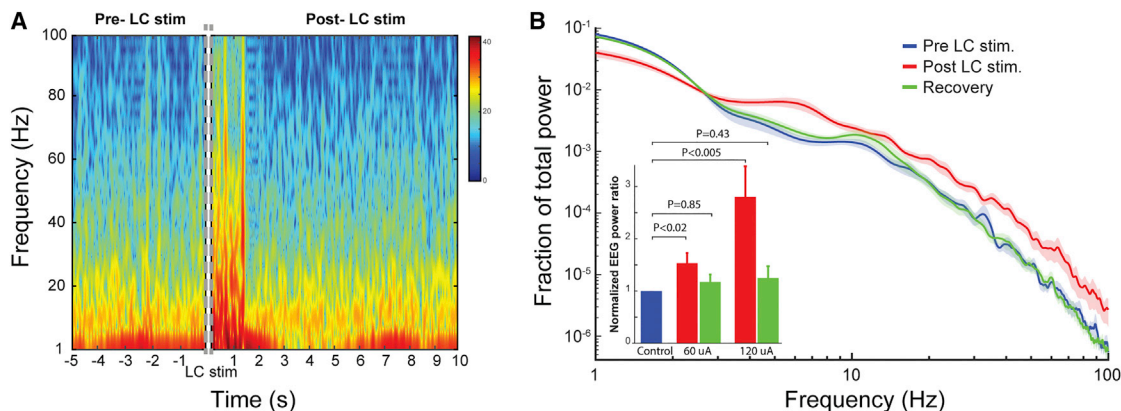


Figure 3. Shift in EEG Power following Phasic LC Stimulation

(A) Example spectrogram of cortical EEG before and after phasic LC stimulation. The dashed gray line indicates the time of phasic LC stimulation. (B) Average fraction of EEG total power versus frequency around LC stimulation. LC stimulations with an amplitude of 60 μ A or 120 μ A both significantly increased the ratio of EEG power in high frequencies (10–100 Hz) to low frequencies (1–10 Hz). Error bars indicate SEM.

dilation in response to phasic LC stimulation were distinct from those in response to tonic stimulation. Tonic LC stimulation generally induced an extended, gradual dilation, whereas phasic LC stimulation induced a rapid, steep increase in pupil size followed by a quick constriction back to the baseline size (Figures 4A and 4B). The lags of the pupil dilation evoked by phasic LC stimulation are 0.83 ± 0.038 and 0.91 ± 0.056 s for ipsilateral and contralateral pupils, respectively, which is comparable with the latency between pupil microdilations and the associated depolarization of transmembrane potentials, as reported in previous work (McGinley et al., 2015a), and the latency between pupil dilation and activation of cortical NE axons (Reimer et al., 2016).

Further, to quantify the time course of the pupil dilations, we calculated time constants for phasic pupil dilations and 5 Hz tonic pupil dilations by fitting an exponential growth curve (Experimental Procedures). Although pupil dilations elicited by 50 Hz phasic LC stimulation were smaller than those elicited by 333 Hz phasic LC stimulation (ipsilateral: $15\% \pm 1\%$ versus $22\% \pm 0.9\%$, $p < 4.8 \times 10^{-5}$; contralateral: $12\% \pm 0.7\%$ versus $20\% \pm 0.9\%$, $p < 3.2 \times 10^{-4}$, Student's t test; Figures S3A and S3B), their time courses were not significantly different (ipsilateral rising: 1.38 ± 0.16 versus 1.31 ± 0.06 s, $p = 0.68$; contralateral rising: 1.38 ± 0.18 versus 1.26 ± 0.07 s, $p = 0.48$; ipsilateral decaying: 4.66 ± 0.62 versus 5.0 ± 0.27 s, $p = 0.64$; contralateral decaying: 4.84 ± 0.89 versus 5.12 ± 0.33 s, $p = 0.71$; Student's t test; Figure S3C). Pupil dilation in response to 5 Hz tonic LC stimulation increased exponentially with time constants of 19.25 ± 3.16 and 29.76 ± 5.80 s for the ipsilateral and contralateral eyes, respectively. In contrast, pupil dilation in response to phasic LC stimulation progressed relatively rapidly. The rising time constant of pupil dilation in response to 5 Hz tonic stimulation was approximately 15-fold larger than that of phasic stimulation for both the ipsilateral (19.25 ± 3.16 versus 1.32 ± 0.058 s, $p < 2 \times 10^{-21}$, Student's t test) and contralateral pupil (29.76 ± 5.80 versus 1.28 ± 0.068 s, $p < 5 \times 10^{-16}$, Student's t test; Figure 4C). The average time constants of the decaying phases of

phasic pupil dilation are 4.95 ± 0.26 and 5.07 ± 0.29 s for the ipsilateral and contralateral eyes, respectively. Because pupil dilations in response to LC tonic stimulation with frequencies of 0.5, 1, and 2 Hz did not typically exhibit an exponential growth curve, we calculated the rising linear slope during 2- to 6-s and 6- to 10-s periods for all tonic stimulation conditions (Figure 4D). In general, the rising slope and size of the evoked dilation was positively correlated with the frequency of tonic stimulation; i.e., higher tonic frequency stimulations generally produced quicker and larger pupil dilations (Figures 4D and 4E).

We next examined what effect background tonic LC activity might have on pupil dilations elicited by phasic LC activity. The percent change of pupil dilation evoked by phasic LC stimulation for both ipsilateral and contralateral eyes exhibited an inverted U profile relative to the increasing frequencies of background tonic LC stimulation. For both the ipsilateral and contralateral pupils, the increase in pupil size after phasic LC stimulation was significantly greater when preceded by 2 Hz tonic LC stimulation than by 5 Hz ($p = 0.01$, Student's t test; for the ipsilateral pupil, $p < 0.03$, Student's t test; for the contralateral pupil, $n = 17$). Moreover, contralateral pupil dilations evoked by phasic LC stimulation were significantly larger in the presence of 2 Hz tonic stimulation than when following no background tonic stimulation ($p < 0.01$, Student's t test). However, this facilitative effect of tonic stimulation on phasic stimulation-induced dilation was only marginally present ($p = 0.06$ Student's t test) for the ipsilateral eye (Figure 4E). Finally, we compared the results from both left ($n = 15$) and right LC stimulation ($n = 2$) and found that they were similar (Figure S4), ruling out the possibility that unilateral LC stimulation-induced lateralized pupil dilation was dependent on which LC was stimulated.

LC Controls Pupil Size Only through the Parasympathetic EWN and Sympathetic SCG

Although previous tracing works have suggested that the LC projects to the EWN, a parasympathetic nucleus controlling the pupillary sphincter muscle via the CG (Breen et al., 1983),

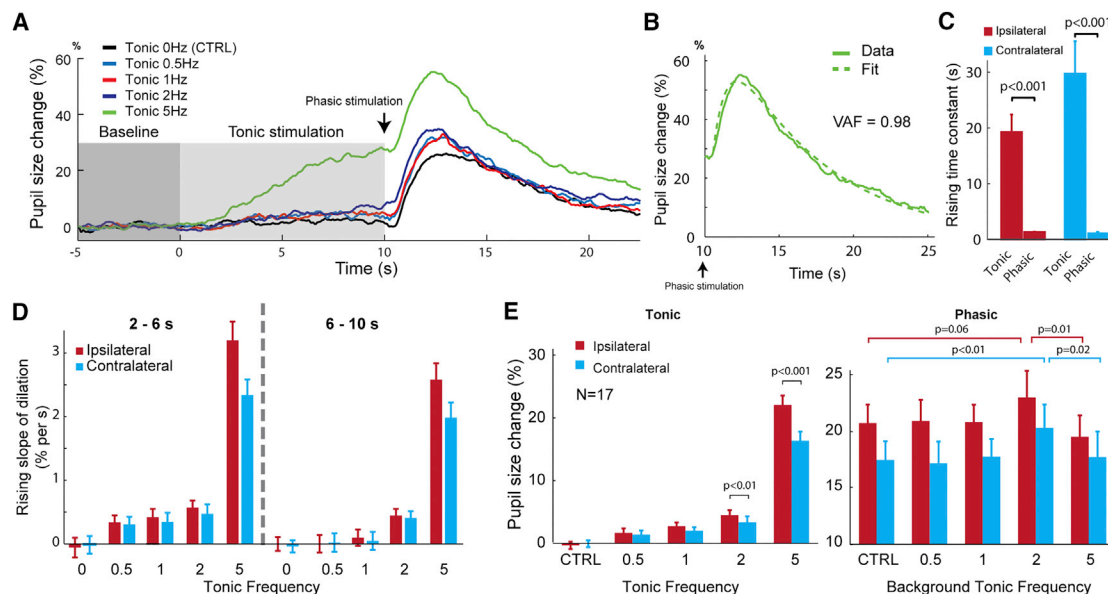


Figure 4. Bilateral Pupil Dilation in Response to Tonic and Phasic Unilateral LC Stimulation

(A) Example change in pupil size (normalized to baseline pupil size) in response to LC activation, with tonic LC stimulation occurring from 0 to 10 s, and phasic stimulation, indicated by the arrow, occurring immediately following tonic stimulation. Each color represents a different tonic stimulation condition.

(B) Pupil dilation following phasic LC stimulation can be well fit with a bi-exponential function.

(C) Average time constant for the rising phase of either ipsilateral or contralateral pupil dilation following either tonic or phasic LC stimulation.

(D) Average rising slope of dilation during each tonic stimulation condition for the ipsilateral and contralateral pupil for the 2- to 6-s and 6- to 10-s period of the tonic stimulation period.

(E) Left: percent of pupil size change during tonic LC stimulation for each tonic stimulation condition in the ipsilateral and contralateral pupils. Both 2 and 5 Hz tonic activation showed a significant cross-eye difference. Right: percent of pupil size change following phasic LC stimulation with different background LC activation for the ipsilateral and contralateral pupils.

Error bars indicate SEM.

and the SCG, a sympathetic nucleus controlling the pupillary dilator muscle (Hancock and Fougousse, 1976), these works did not rule out the possibility that the LC affects pupil size through additional pathways (Figure 5A). To test whether the LC modulates pupil size through nuclei other than the EWN and SCG, we pharmacologically blocked the influence of the LC on the EWN by injecting $\sim 1 \mu\text{L}$ yohimbine, an α -2 receptor antagonist, into the ipsilateral EWN. Fluorescent dye mixed with the yohimbine solution confirmed that the spread of yohimbine solution was limited to $\sim 250 \mu\text{m}$ from the injection site (Figure 5B). At the same time, we performed an SCGx; i.e., surgical removal of the SCG. Immunohistochemistry confirmed the identity of the removed tissue by showing that its cells expressed both neurofilaments and tyrosine hydroxylase, hallmarks of sympathetic neurons (Savastano et al., 2010; Figure 5C). In concert with SCGx, the pharmacological blockage of α -2 receptors in the EWN with 1 mM yohimbine eliminated the pupil dilation in response to phasic LC activation (Figure 5D, dark traces), whereas 0.5 mM yohimbine only partially diminished pupil dilation in response to LC activation (Figure 5D, gray trace). Pupillary responses to LC stimulation started to reappear 1 hr after the injection. Taken together, the dose-dependent reduction and re-appearance of LC activation-evoked pupillary responses following a recovery period suggest that the observed inactivation was due to the injection of yohimbine. Thus, this confirmed

that the EWN and SCG were essential to the pupillary response to LC activation.

Lateralization of Pupil Dilation in Response to LC Stimulation Is Due to a Unilateral Sympathetic Pathway

Although unilateral LC stimulation induced bilateral pupil dilation, normalized dilation of the ipsilateral pupil, was significantly larger than that of the contralateral pupil in response to both 2 and 5 Hz tonic and phasic LC stimulation (tonic 5 Hz: 0.22 ± 0.015 versus 0.16 ± 0.014 , $p < 0.001$, paired Student's t test; tonic 2 Hz: 0.05 ± 0.008 versus 0.034 ± 0.009 , $p = 0.002$, paired Student's t test; phasic: 0.211 ± 0.008 versus 0.181 ± 0.008 , $p < 3 \times 10^{-13}$, paired Student's t test (Figures 4E and 6A). This suggests that LC activity may affect the ipsilateral and contralateral pupils differently through the sympathetic and parasympathetic pathways, producing this pronounced lateralization.

The difference between the dilation of the ipsilateral and contralateral pupils was quantified as a lateralization ratio, defined as the normalized change in pupil size for the ipsilateral pupil divided by that for the contralateral pupil. We only analyzed the lateralization ratios for 2 and 5 Hz tonic stimulation because the marginal pupil dilations induced by stimulations at < 2 Hz resulted in unreliable estimation of the lateralization ratios.

For almost all animals, tonic LC stimulation induced a significantly larger ipsilateral than contralateral pupil dilation, resulting

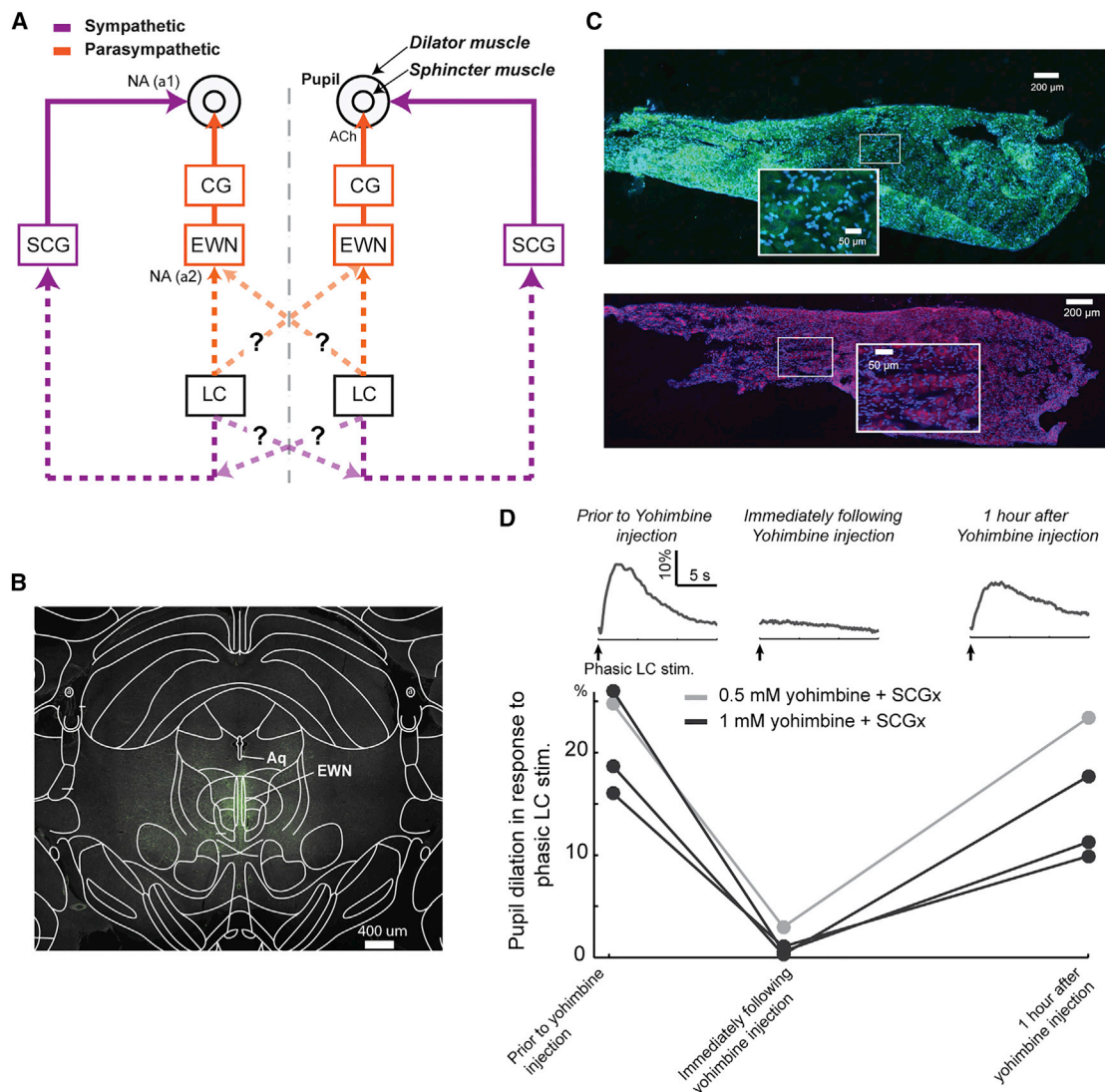


Figure 5. The Sympathetic SCG and Parasympathetic EWN Nuclei Are Essential for the LC to Modulate Pupil Size

(A) Although the literature suggests that the LC modulates ipsilateral pupil size through both a sympathetic (LC→IML→SCG→dilator muscle) and parasympathetic (LC→EWN→CG→sphincter muscle) pathway, the pathway through which the LC modulates contralateral pupil size remains unclear (question marks indicate other possible pathways).

(B) Histological confirmation that the yohimbine and dye injection spread throughout the EWN (overlaid brain atlas aligned by aqueduct location).

(C) Immunohistochemical identification of an SCG that was surgically removed through SCGx. Neurofilaments and tyrosine hydroxylase are labeled green and purple, respectively, and blue DAPI labels cell nuclei. The area within the white box is shown at 40× magnification to show labeling at a cellular scale.

(D) The effects of blocking alpha-2 receptors in the EWN with 0.5 and 1 mM yohimbine on phasic LC stimulation-induced pupil dilations.

in a lateralization ratio of 1.45 ± 0.1 ($p < 2 \times 10^{-4}$, Student's *t* test, mean \pm SEM). When the percent change in pupil size was plotted for the ipsilateral eye versus the contralateral eye, the vast majority of the data points fell below the unity line (Figure 6A). Interestingly, the lateralization ratios for 2 Hz were slightly but not significantly larger than 5 Hz ($p = 0.91$, Student's *t* test), although pupil dilation was larger for 5 Hz than 2 Hz (Figure 6A, inset).

We next examined the extent to which the sympathetic and parasympathetic pathways contribute to the pupil dilation evoked by LC activation. We found that unilateral LC stimulation evoked bilateral pupil dilation with lateralization. However, it is

unclear whether this lateralization was due to bilateral LC projections to either the sympathetic or parasympathetic pathways or through a combination of both. Moreover, because pupil size has been shown to tightly co-vary with level of arousal (McGinley et al., 2015a; Nassar et al., 2012; Reimer et al., 2014; Vinck et al., 2015), which involves both the sympathetic and parasympathetic nervous systems, we wanted to further tease apart the contribution of these systems to pupil dilation in response to LC activation. To this end, we performed an SCGx to remove either the ipsilateral or contralateral SCG, a part of the sympathetic pathway from the LC to the dilator pupillae muscle. To our surprise,

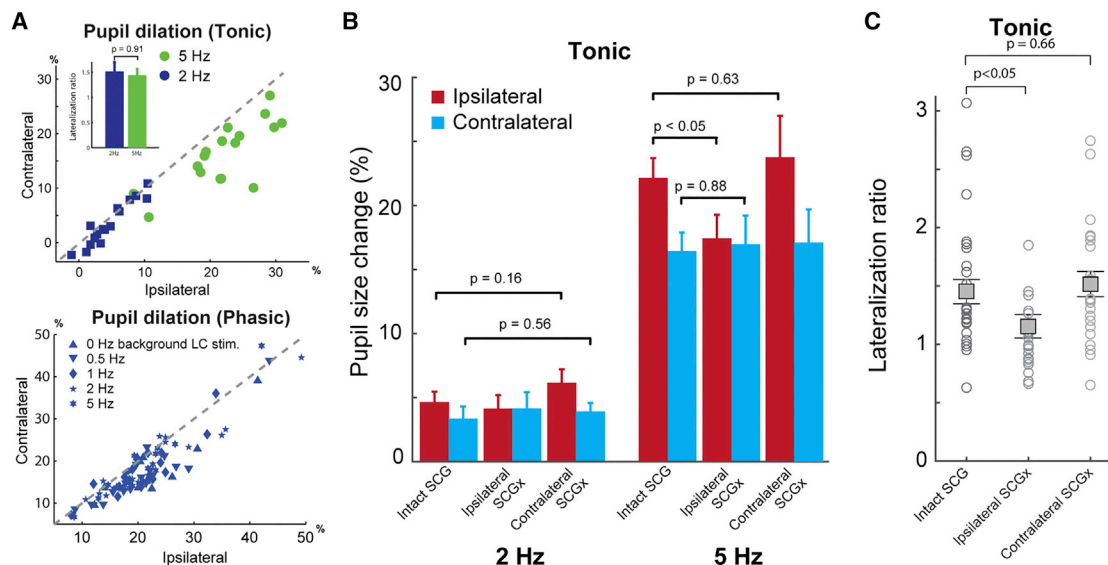


Figure 6. Ipsilateral or Contralateral SCGx Allowed Us to Tease Apart the Individual Contributions of the Sympathetic and Parasympathetic Pathways

(A) Top: percent of pupil size change during 2 and 5 Hz tonic LC stimulation in the ipsilateral versus contralateral pupil. Inset: the mean lateralization ratio of pupil dilation in response to 2 and 5 Hz tonic LC stimulation. The dashed line is the unity line. Bottom: percent of pupil size change during phasic LC stimulation following various tonic LC stimulation conditions in the ipsilateral versus contralateral pupil.

(B) Contralateral SCGx had no effect on bilateral pupil dilation in response to 2 and 5 Hz tonic LC stimulation, whereas ipsilateral SCGx resulted in significantly diminished 5-Hz-evoked ipsilateral but not contralateral dilation.

(C) Ipsilateral SCGx resulted in a decrease in the mean lateralization ratio for 2 and 5 Hz LC stimulation, whereas contralateral SCGx did not affect the lateralization ratio.

Error bars indicate SEM.

contralateral SCGx did not induce any significant change in pupil dilations in response to tonic LC stimulation for either the ipsilateral or contralateral pupils ($p > 0.16$ for the ipsilateral pupil and $p > 0.56$ for the contralateral pupil, Mann-Whitney U test; Figure 6B), nor did it induce any significant change in the lateralization ratio when compared with data collected with an intact SCG (1.45 ± 0.1 versus 1.51 ± 0.11 , $p = 0.66$, Mann-Whitney U test; Figure 6C). This suggests that LC activation affects the size of the contralateral pupil only through lateral projections to the parasympathetic pathway. In line with this hypothesis, ipsilateral SCGx significantly reduced pupil dilation in response to tonic LC stimulation for ipsilateral pupils (0.22 ± 0.015 versus 0.17 ± 0.016 , $p = 0.026$, Mann-Whitney U test), but this change was not seen in contralateral pupils (0.16 ± 0.014 versus 0.16 ± 0.018 , $p = 0.88$, Mann-Whitney U test) (Figure 6B). Moreover, ipsilateral SCGx resulted in the mean lateralization ratio for 2 and 5 Hz LC stimulation significantly diminishing, from 1.45 ± 0.1 to 1.15 ± 0.1 ($p = 0.048$, Student's t test; Figure 6C), indicating that the sympathetic pathway substantially contributed to pupil dilation induced by unilateral LC activation only for the ipsilateral eye.

Contribution of the Sympathetic Pathway Is Dependent on the Frequency of LC Activation, whereas Parasympathetic Contribution Is Not

Our data have suggested that the lateralization of pupil dilation in response to LC stimulation is mainly due to unilateral projection of the LC through the sympathetic pathway. In addition, the lateral-

ization ratio of pupil dilation following phasic LC stimulation was significantly less than that following tonic LC stimulation (Figure 7A; $p < 0.001$, Student's t test). Interestingly, for phasic LC stimulation, although contralateral SCGx had no effect on the lateralization ratio, ipsilateral SCGx also failed to significantly diminish the lateralization ratio (Figure 7B). Taken together, this leads us to hypothesize that the relative contribution of the ipsilateral sympathetic pathway to LC activation-evoked pupil dilation was dependent on the frequency of LC activation. Indeed, when we compared the lateralization ratio of pupil dilation across different LC stimulation frequencies in animals with an intact SCG, we observed that the lateralization ratio decreased as the frequency of LC stimulation increased. This contrasts with the relatively constant lateralization ratio seen across the same stimulation frequencies in rats with ipsilateral SCGx (Figure 7B). We could then examine the contribution of the ipsilateral sympathetic and parasympathetic pathways relative to the contralateral parasympathetic pathway because ipsilateral SCGx eliminated the sympathetic influence of LC stimulation on the ipsilateral pupil's dilation (Figure 7C), allowing us to isolate the contribution of the parasympathetic pathway to the pupils' dilations. Because we have confirmed that the LC modulates pupil dilation only through the sympathetic SCG and parasympathetic EWN (Figure 5D), we were able to determine the relative contribution of the sympathetic pathway by subtracting the mean lateralization ratio in rats that received ipsilateral SCGx from that of rats with an intact SCG. This calculation unveiled the logarithmic relationship

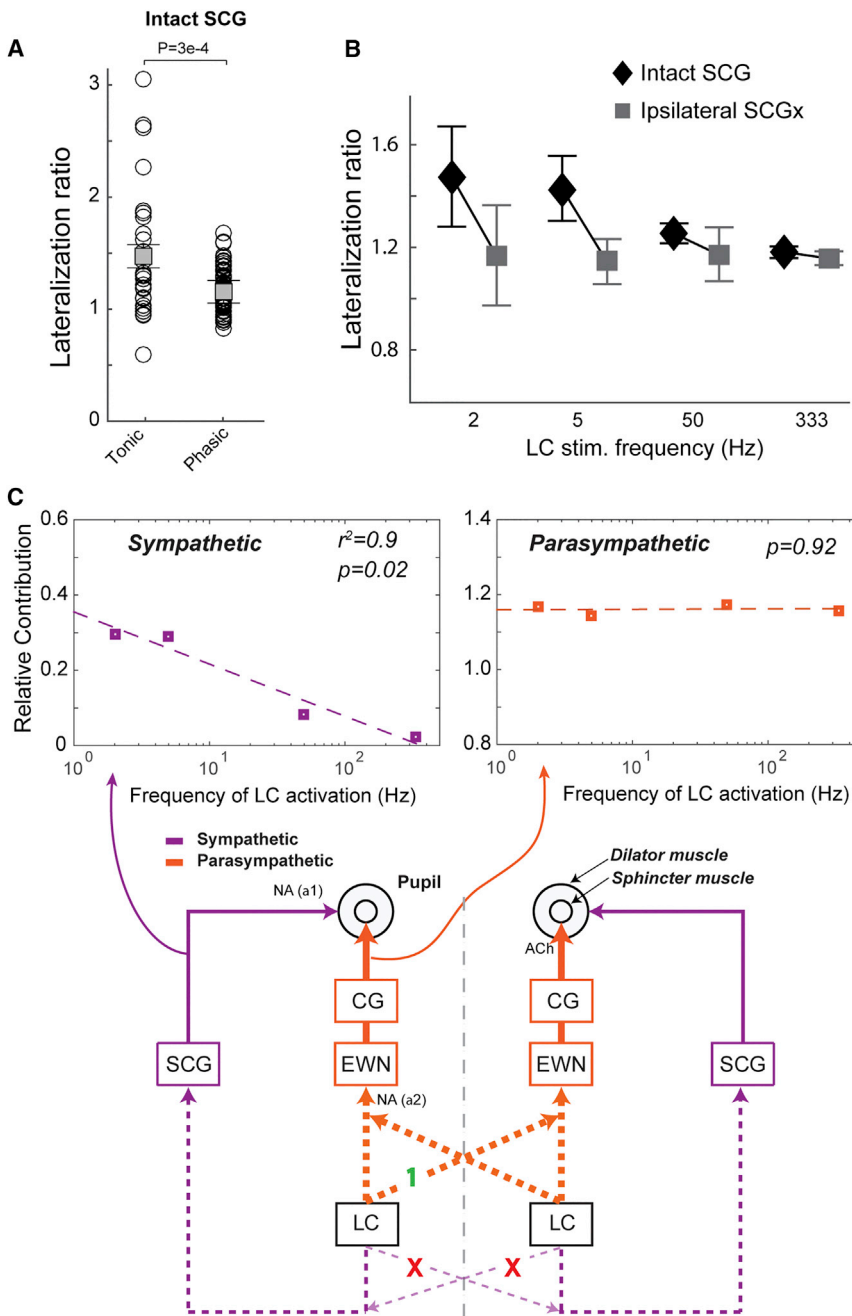


Figure 7. The Relative Contribution of the Sympathetic, but Not Parasympathetic, Pathway Depends on the Frequency of LC Activation

(A) The lateralization ratio for tonic LC stimulation in animals with intact SCGs.

(B) Lateralization ratio of pupil dilation evoked by different LC stimulations in both animals with intact SCGs and with ipsilateral SCGx. The differences in the lateralization ratio between SCG-intact animals and ipsilateral SCGx animals reflects the relative contribution of the sympathetic pathway.

(C) The LC modulates the size of the contralateral pupil only through a lateral projection to the contralateral parasympathetic system (Xs indicate disproved potential pathways). The relative contribution of the sympathetic pathway exponentially decayed with increasing frequency of LC activation, whereas the relative contribution of the parasympathetic pathway was insensitive to the frequency. All contributions were normalized by the contribution from the LC to the contralateral parasympathetic pathway (green 1). Error bars indicate SEM.

about how LC activity influences pupil size besides recent work conclusively establishing the causal link between LC activation and pupil dilation (Joshi et al., 2016). We show that unilateral LC activation evoked bilateral dilation. Further, we found an across-eye difference in the size of the evoked bilateral dilation, indicating a lateralization in the pathways between the LC and both pupils. The degree of this lateralization was found to be greater for dilations in response to tonic LC stimulation compared with phasic LC stimulation-evoked dilations, indicating that the across-eye difference depends on the frequency of LC activation. Next, through pharmacological and surgical blocking of the EWN and SCG, we demonstrate that the LC influences pupil size only through two pathways, a parasympathetic pathway through the EWN and a sympathetic pathway through the

SCG. Finally, by performing ipsilateral or contralateral SCGx, we found that the LC influences the ipsilateral pupil through both parasympathetic and sympathetic pathways but influences the contralateral pupil only through the parasympathetic pathway. Therefore, differences between bilateral pupil dilations were mainly attributed to sympathetic contribution, suggesting that a measurement of across-eye differences in bilateral pupil dilation may present itself as a biomarker for abnormal autonomic activities, such as those observed in neuropsychiatric disorders (Eilam-Stock et al., 2014; Fujibayashi et al., 2009). Here we discuss these findings in the context of previous studies in

DISCUSSION

Although the LC has been hypothesized for decades to modulate changes in pupil size during behavioral tasks, very little is known

which pupil size was used to index neural computation and cognitive processing.

In this project, we used an anesthetized rat model instead of an awake animal model for several reasons. First, our data suggested that there is no significant difference in LC-mediated changes between lightly isoflurane-anesthetized animals and head-constrained idle (i.e., no behavioral tasks) animals (Figure S1). Second, the anesthesia allowed us to carefully characterize pupil dilation in response to different LC activation frequencies (five tonic frequencies in combination with a phasic frequency), which entails prolonged pupil recording procedures (~3–5 hr). To the best of our knowledge, this duration is well beyond the limits for which the animals can tolerate head fixation. Finally, to tease apart the contributions of the sympathetic pathway, we performed SCGx to block the sympathetic pathway. SCGx, however, typically results in a blepharoptosis, causing the eyelid to occlude the pupil. In our anesthetized setup, we used eyelid retractors to gently hold open the eyelids after SCGx. However, in an awake setup, there is no humane way to open animals' eyelids during blepharoptosis.

Pupil dilation may reflect the activity of an arousal network affecting multiple brain structures (Aston-Jones and Cohen, 2005; Eldar et al., 2013; Hermans et al., 2011; Joshi et al., 2016). For example, Joshi et al. (2016) unexpectedly found that the activation of multiple brain structures, including the LC, superior colliculus, inferior colliculus, and cingulate cortex, elicited pupil dilation. In this work, we focused on elucidating only the mechanisms through which LC mediates pupil dilations. Although anesthesia has allowed us to do so with minimal background noises from the other pupil dilation-evoking brain structures, it remains important to characterize the complex interplay between the LC and other arousal-related brain structures in collectively mediating pupil dilation. This will necessitate further work in awake behaving animals.

Consistent with previous work, our data showed that LC stimulation evoked pupil dilation. Moreover, unilateral LC stimulation evoked pupil dilation for both eyes but with lateralization. One possible explanation for this result may be found in previous work, which has shown that electrical stimulation of a single LC nucleus results in activation of the corresponding contralateral LC (Marzo et al., 2014). Although this finding is very interesting, and the existence of lateral projections between the two LCs remains unclear (Li et al., 2016; Luppi et al., 1995), for the following reasons, we believe indirect activation of the contralateral LC is not likely to be the cause of the bilateral pupil dilation observed in our experiments. First, the intensity we used for electrical microstimulation was substantially lower than the current threshold necessary for eliciting contralateral LC activity, as reported in previous work (Marzo et al., 2014). Second, if bilateral dilation resulting from unilateral LC stimulation was due to bilateral LC activation, then surgically blocking the sympathetic pathway to the contralateral pupil would result in a decrease in dilation for the contralateral pupil. However, our data demonstrated that this is not the case. The LC has been shown to make bilateral projections into many brain regions (Simpson et al., 1997; Steindler, 1981). For example, Simpson et al. (1997) found that each LC bilaterally projects to different stages along the somatosensory pathway, with a relatively small differ-

ence in projection density in the brain stem and a large difference in the cortex. Consistent with this notion, our data suggest that the LC exhibits bilateral influence over both EWNs in the brain stem, with little difference in relative strength, given that our calculated lateralization ratio for the parasympathetic pathway (~1.15) is close to unity.

Lateralization is ubiquitous in sensory processing and executive functions. For instance, information about tactile grating orientations is processed in the left hemisphere, whereas information about grating locations is processed in the right hemisphere (Van Boven et al., 2005). Similarly, visuospatial attentional tasks dominantly engage the right hemisphere (Thiebaut de Schotten et al., 2011). Although the LC is interconnected with various brain regions, it remains unclear whether lateralized information processing differentially involves the bilateral LCs. As our data suggested, if there is a lateralization in the involvement of the bilateral LCs in any process, then it should be evidenced by lateralized pupil dilation. Indeed, a recent work reported that there was a systematic lateralization in pupil sizes in human subjects performing an attentional task. This lateralization became evident in the second and third session of the task and increased with attentional load, suggesting that it was co-modulated by the attentional load and arousal associated with task experience (Wahn et al., 2017). Consistent with this work, electrodermal activity-linked arousal also exhibits lateralization (Picard et al., 2016). Future non-invasive neural imaging work remains to be done to test whether this lateralization in changes in pupil size is due to bilateral differences in LC activation (de Gee et al., 2017; Murphy et al., 2014; Payzan-LeNestour et al., 2013).

"Microdilations," with similar properties as our phasic LC-activation-induced dilations, have been observed to frequently occur in the pupils of awake behaving rodents (McGinley et al., 2015a). These microdilations follow an archetypical temporal shape: an initial, rapid increase in pupil size with an approximately 2-s time course followed by a slower constriction back to baseline size. We found phasic LC-activation-evoked dilations exhibited a qualitatively similar temporal shape, with time constants of 1.28 and 1.32 s for rise (ipsilateral and contralateral pupil, respectively) and 4.95 and 5.07 s for decay (ipsilateral and contralateral pupil, respectively). These similarities suggest that microdilations may be a good indicator of LC phasic firing, providing a physiological relevance to their correlation with arousal. An intriguing property of the microdilations was their high correlation with a transient depolarization of membrane potentials of cortical neurons, with microdilations occurring approximately 1 s after depolarizations (McCormick et al., 2015). Similarly, in our data, pupil dilation had an average onset time of 0.83 and 0.91 s (ipsilateral and contralateral pupil, respectively) following phasic activation of the LC. Previous work has shown that NE release from LC projections depolarizes the membrane potential of neurons by reducing resting potassium conductance (McCormick and Pape, 1990; McCormick and Prince, 1988). Therefore, consistent with previous experimental results, our data suggest that the correlation between microdilations and the depolarization of cortical membrane potentials may result from common LC input.

Slow fluctuations in baseline pupil size and rapid, transient pupil dilations are thought to encode non-redundant information

about cognitive processes. For instance, [de Gee et al. \(2014\)](#) demonstrated that, in a protracted perceptual decision process, in addition to a transient pupil dilation associated with the final behavioral choice, there were sustained, relatively slow changes in pupil size throughout the decision formation period. In a separate study, in a predictive inference task, [Nassar et al. \(2012\)](#) found that transient pupil dilation correlated with the level of unexpected uncertainty, whereas average pupil size correlated with the level of expected uncertainty, leading them to hypothesize that these important properties of internal models may be represented by the tonic and phasic modes of LC activation, respectively. In strong support of this idea, our data indicated that tonic and phasic LC activation resulted in pupil dilations with disparate characteristics. For both eyes, tonic LC activation induced relatively weak and slow pupil dilations, whereas phasic LC activation resulted in strong but transient pupil dilations.

Attempts have previously been made to infer the individual contributions of the parasympathetic and sympathetic pathways to task-evoked pupil dilations by pharmacologically blocking the dilator or sphincter muscles separately during cognitive tasks ([Steinhauer et al., 2004](#)). Blocking the dilator muscle was found to have a weaker effect on pupil dilations as compared with blocking the sphincter muscle, suggesting that the sympathetic pathway less strongly modulates pupil size. Our data quantified the contribution of the sympathetic pathway to pupil dilation relative to the parasympathetic pathway with a ratio of approximately 0.36:1 and 0.09:1 for tonic and phasic LC activation, respectively. This supports the notion that phasic pupil dilation is mainly due to central inhibition of parasympathetic preganglionic neurons through the EWN in the midbrain.

The LC remains a challenge to study because it is relatively inaccessible because of its small size and deep location in the brain stem. A model by which LC activation can be inferred from non-luminance-induced changes in pupil size may benefit the community studying this important brain structure. Revealing the neural mechanisms by which the LC modulates pupil size is a step toward the development of such a model.

EXPERIMENTAL PROCEDURES

Surgery and Electrophysiology

All procedures were approved by the Columbia University Institutional Animal Care and Use Committee and were in agreement with NIH guidelines. 56 Sprague-Dawley rats (225–300 g, 53 females, $n = 50$ for acute experiments, $n = 6$ for behavior) were used for these experiments. The acute procedures were similar to those previously described in detail ([Wang et al., 2012](#); [Zheng et al., 2015](#)). Animals were anesthetized with isoflurane (1%–2%). After craniotomy, a tungsten microelectrode (1–2 M Ω , FHC, Inc.) was advanced to the LC using a hydraulic microdrive ([Wang et al., 2010](#)). LC activity was determined based on wide spike waveform, response to a paw pinch, and other criteria used in previous studies ([Supplemental Experimental Procedures](#)). EEG signals between a contralateral frontal cortex screw and a screw over the contralateral occipital cortex were differentially amplified and recorded, along with extracellular neural signals using a Plexon system.

For chronic implantations, a sterile platinum/iridium microelectrode (~1 M Ω , FHC, Inc.) was advanced to the LC, bonded to a head plate using dental cement, and connected to a connector cemented in the head cap ([Figure S1](#)).

SCGx

The SCG was removed on either the right ($n = 12$) or the left ($n = 13$) side before craniotomy using a procedure described in detail previously ([Savastano et al.,](#)

[2010](#)). A vertical incision along the midline was made to expose the mandibular glands. The sternohyoid and omohyoid muscles were carefully separated to expose the lymph node and carotid artery. At the bifurcation of the carotid artery, the external and internal carotid artery were carefully separated from the SCG underneath. The pre- and post-ganglion branches of the SCG were cut to allow for its removal, followed by its fixation in 4% paraformaldehyde for immunohistochemistry.

Pupillometry Recording

Recordings of both pupils were made using two pupillometry systems triggered by a real-time system with data streamed to hard drives. For LC stimulation experiments, the eyelids of the animal were gently held open by eyelid retractors, and artificial eye drops were used to hydrate the corneas. Images of both pupils were collected at 50 Hz.

Pupillary light reflex was measured in 4 acute experiments in which left pupillary responses to switching of ambient illuminance between 15 and 150 lux every 20 s were recorded. The same measurement was also performed in three awake, head-fixed animals after they became habituated to head fixation ([Bari et al., 2013](#); [Ollerenshaw et al., 2012, 2014](#)).

LC Microstimulation

Biphasic current pulses (cathode-leading, 200 μ s per phase) were delivered by a calibrated electrical microstimulator (Multi Channel Systems, or PSU6/S88, Grass Instrument) to activate the LC. In acute setups, current pulses (60 μ A) were used to evoke pupil dilation. Each stimulus block consisted of 5 s of baseline followed by 10 s of tonic LC stimulation with different frequencies (0, 0.5, 1, 2, and 5 Hz), which was then followed by phasic LC stimulation (50 Hz or 330 Hz, 6 pulses). These stimulus blocks ([Figure 3A](#)) were delivered in an interleaved fashion with 60 s between each block. In awake setups, current pulses (50 Hz, 6 pulses, 150 μ A) were delivered to an implanted LC electrode every 60–120 s, with a random delivery of a drop of Kool-Aid solution occurring 20–40 s prior.

Immunohistochemistry

The animal's brain was sectioned coronally at 20 μ m using a freezing microtome (Leica Microsystems). Standard Nissl staining was used to verify placement of the electrode tip in the LC. Sections were examined using an Olympus CKX41 microscope.

SCG cells were labeled with tyrosine hydroxylase and neurofilament antibodies to confirm their sympathetic and neuronal identity, respectively. SCGs were sectioned in the longitudinal direction at 10 μ m using the freezing microtome, and sections were mounted onto two separate microscope slides for immunodetection of neurofilament-containing cells and tyrosine hydroxylase-containing neurons using different antibodies ([Supplemental Experimental Procedures](#)). Sections were imaged on an Olympus FV-1000 confocal microscope.

Data Analysis

To quantify the shift of EEG power, Welch's power spectral density estimate was used to calculate the ratio of power between 10–100 Hz to power between 1–10 Hz. This ratio was calculated for the 4-s segment before LC stimulation, the 4-s segment after LC stimulation, and the 4-s second segment lasting from 4 to 8 s after LC stimulation, referred to as the recovery period.

Pupil contour was segmented by estimating a histogram of pixel intensity, which allows for calculation of the optimal threshold to extract pupil contour ([Otsu, 1979](#)). In acute setups, a small subset of trials (<10% of the total trials) during which pupil size exceeded 250% of the baseline or fell beneath 40% of the baseline for >2 s were excluded from the analysis. In awake setups, pupil size during blinks (<2% of frames) was linearly interpolated using values from before and after each blink. Pupil size was low pass-filtered (cutoff frequency, 3.75 Hz). The change in pupil size was then calculated for each trial by subtracting the mean baseline pupil size and subsequently dividing by the mean pupil size.

The time constants of the pupillary light reflex were evaluated by fitting exponential rising and decaying curves, respectively, as $y = A + B(1 - e^{-t/\tau_r})$

$$y = A + Be^{-\frac{t}{\tau_d}}$$

where τ_d and τ_c are the time constants of the rising and decaying curves, respectively. A is the baseline pupil size, and B is the amplitude of change in pupil size induced by switching ambient illuminance.

To estimate the time constant of transient pupil dilation in response to LC stimulation, the change in pupil size following phasic stimulation was fit with a bi-exponential curve as

$$y = Ae^{-\frac{t}{\tau_d}} - (A - y(0))e^{-\frac{t}{\tau_r}},$$

where τ_r and τ_d are the time constants of the rising and decaying phases, respectively; $y(0)$ is the initial value of the bi-exponential curve; and A is the amplitude. Only estimated time constants with a variance accounted for (VAF) > 0.9 were used in the comparison between phasic and 5 Hz tonic stimulation (Figure 3D). Phasic pupil dilation amplitude was defined as the difference between the maximum pupil size within 5-s after phasic stimulation and the pupil size at the onset of the phasic dilation.

To estimate the time constant of pupil dilation in response to tonic 5 Hz LC stimulation, the change in pupil size was fit with an exponential rise curve as

$$y = A \left(1 - e^{-\frac{t}{\tau_i}} \right),$$

where τ_i is the curve's time constant. Only estimated time constants with a VAF > 0.9 were used in the comparison between phasic and 5 Hz tonic stimulation. The pupil size change evoked by 2 and 5 Hz tonic stimulation was defined as the mean normalized change in pupil size during the last 2 s.

Statistics

A one-sample Kolmogorov-Smirnov test (MATLAB function kstest) was used to assess the normality of data before performing statistical tests. If the samples were normally distributed, then Student's *t* test was used. Otherwise, Mann-Whitney *U* test was used for unpaired samples or Wilcoxon signed-rank test for paired samples. Tukey's post hoc test was performed for all multiple comparisons.

SUPPLEMENTAL INFORMATION

Supplemental Information includes Supplemental Experimental Procedures and four figures and can be found with this article online at <http://dx.doi.org/10.1016/j.celrep.2017.08.094>.

AUTHOR CONTRIBUTIONS

Q.W. conceived the study. Y.L. and Q.W. designed the experiments. Y.L., C.R., B.S., and Q.W. performed the experiments. Y.L. and N.M. performed the histological analysis. Q.W. and C.R. analyzed the data, and Y.L., C.R., and Q.W. wrote the paper. All authors commented on the manuscript.

ACKNOWLEDGMENTS

We would like to thank Dr. J.M. Alonso and Dr. R. Bruno for their comments at various points of this work. This work is supported by NIH R01MH112267.

Received: January 9, 2017

Revised: July 25, 2017

Accepted: August 28, 2017

Published: September 26, 2017

REFERENCES

Andreassi, J.L. (2006). Pupillary response and behavior. In *Psychophysiology: Human Behavior & Physiological Response*, J.L. Andreassi, ed. (Psychology Press), pp. 289–307.

Aston-Jones, G., and Bloom, F.E. (1981). Norepinephrine-containing locus coeruleus neurons in behaving rats exhibit pronounced responses to non-noxious environmental stimuli. *J. Neurosci.* *1*, 887–900.

Aston-Jones, G., and Cohen, J.D. (2005). An integrative theory of locus coeruleus-norepinephrine function: adaptive gain and optimal performance. *Annu. Rev. Neurosci.* *28*, 403–450.

Aston-Jones, G., Chiang, C., and Alexinsky, T. (1991). Discharge of noradrenergic locus coeruleus neurons in behaving rats and monkeys suggests a role in vigilance. *Prog. Brain Res.* *88*, 501–520.

Aston-Jones, G., Rajkowski, J., Kubiak, P., and Alexinsky, T. (1994). Locus coeruleus neurons in monkey are selectively activated by attended cues in a vigilance task. *J. Neurosci.* *14*, 4467–4480.

Aston-Jones, G., Rajkowski, J., Kubiak, P., Valentino, R.J., and Shipley, M.T. (1996). Role of the locus coeruleus in emotional activation. *Prog. Brain Res.* *107*, 379–402.

Bari, B.A., Ollerenshaw, D.R., Millard, D.C., Wang, Q., and Stanley, G.B. (2013). Behavioral and electrophysiological effects of cortical microstimulation parameters. *PLoS ONE* *8*, e82170.

Berridge, C.W., and Foote, S.L. (1991). Effects of locus coeruleus activation on electroencephalographic activity in neocortex and hippocampus. *J. Neurosci.* *11*, 3135–3145.

Berridge, C.W., and Waterhouse, B.D. (2003). The locus coeruleus-noradrenergic system: modulation of behavioral state and state-dependent cognitive processes. *Brain Res. Brain Res. Rev.* *42*, 33–84.

Bouret, S., and Richmond, B.J. (2015). Sensitivity of locus coeruleus neurons to reward value for goal-directed actions. *J. Neurosci.* *35*, 4005–4014.

Breen, L.A., Burde, R.M., and Loewy, A.D. (1983). Brainstem connections to the Edinger-Westphal nucleus of the cat: a retrograde tracer study. *Brain Res.* *261*, 303–306.

Chapman, C.R., Oka, S., Bradshaw, D.H., Jacobson, R.C., and Donaldson, G.W. (1999). Phasic pupil dilation response to noxious stimulation in normal volunteers: relationship to brain evoked potentials and pain report. *Psychophysiology* *36*, 44–52.

Clayton, E.C., Rajkowski, J., Cohen, J.D., and Aston-Jones, G. (2004). Phasic activation of monkey locus coeruleus neurons by simple decisions in a forced-choice task. *J. Neurosci.* *24*, 9914–9920.

de Gee, J.W., Knapen, T., and Donner, T.H. (2014). Decision-related pupil dilation reflects upcoming choice and individual bias. *Proc. Natl. Acad. Sci. USA* *111*, E618–E625.

de Gee, J.W., Colizoli, O., Kloosterman, N.A., Knapen, T., Nieuwenhuis, S., and Donner, T.H. (2017). Dynamic modulation of decision biases by brainstem arousal systems. *eLife* *6*, e23232.

Devilbiss, D.M., and Waterhouse, B.D. (2011). Phasic and tonic patterns of locus coeruleus output differentially modulate sensory network function in the awake rat. *J. Neurophysiol.* *105*, 69–87.

Ebitz, R.B., Pearson, J.M., and Platt, M.L. (2014). Pupil size and social vigilance in rhesus macaques. *Front. Neurosci.* *8*, 100.

Ego-Stengel, V., Bringuier, V., and Shulz, D.E. (2002). Noradrenergic modulation of functional selectivity in the cat visual cortex: an in vivo extracellular and intracellular study. *Neuroscience* *111*, 275–289.

Eilam-Stock, T., Xu, P., Cao, M., Gu, X., Van Dam, N.T., Anagnostou, E., Kolevzon, A., Soorya, L., Park, Y., Siller, M., et al. (2014). Abnormal autonomic and associated brain activities during rest in autism spectrum disorder. *Brain* *137*, 153–171.

Eldar, E., Cohen, J.D., and Niv, Y. (2013). The effects of neural gain on attention and learning. *Nat. Neurosci.* *16*, 1146–1153.

Ersen, A., Elkabes, S., Freedman, D.S., and Sahin, M. (2015). Chronic tissue response to untethered microelectrode implants in the rat brain and spinal cord. *J. Neural Eng.* *12*, 016019.

Fujibayashi, M., Matsumoto, T., Kishida, I., Kimura, T., Ishii, C., Ishii, N., and Moritani, T. (2009). Autonomic nervous system activity and psychiatric severity in schizophrenia. *Psychiatry Clin. Neurosci.* *63*, 538–545.

- Hancock, M.B., and Fougereuse, C.L. (1976). Spinal projections from the nucleus locus coeruleus and nucleus subcoeruleus in the cat and monkey as demonstrated by the retrograde transport of horseradish peroxidase. *Brain Res. Bull.* 7, 229–234.
- Hermans, E.J., van Marle, H.J.F., Ossewaarde, L., Henckens, M.J.A.G., Qin, S., van Kesteren, M.T.R., Schoots, V.C., Cousijn, H., Rijpkema, M., Oostenveld, R., and Fernández, G. (2011). Stress-related noradrenergic activity prompts large-scale neural network reconfiguration. *Science* 334, 1151–1153.
- Hirata, A., Aguilar, J., and Castro-Alamancos, M.A. (2006). Noradrenergic activation amplifies bottom-up and top-down signal-to-noise ratios in sensory thalamus. *J. Neurosci.* 26, 4426–4436.
- Hong, L., Walz, J.M., and Sajda, P. (2014). Your eyes give you away: prestimulus changes in pupil diameter correlate with poststimulus task-related EEG dynamics. *PLoS ONE* 9, e91321.
- Joshi, S., Li, Y., Kalwani, R.M., and Gold, J.I. (2016). Relationships between Pupil Diameter and Neuronal Activity in the Locus Coeruleus, Colliculi, and Cingulate Cortex. *Neuron* 89, 221–234.
- Kalwani, R.M., Joshi, S., and Gold, J.I. (2014). Phasic activation of individual neurons in the locus coeruleus/subcoeruleus complex of monkeys reflects rewarded decisions to go but not stop. *J. Neurosci.* 34, 13656–13669.
- Li, Y., Hickey, L., Perrins, R., Werlen, E., Patel, A.A., Hirschberg, S., Jones, M.W., Salinas, S., Kremer, E.J., and Pickering, A.E. (2016). Retrograde optogenetic characterization of the pontospinal module of the locus coeruleus with a canine adenoviral vector. *Brain Res.* 1641 (Pt B), 274–290.
- Lowenstein, O., and Loewenfeld, I.E. (1962). The Pupil. In *The Eye*, H. Davson, ed. (New York: Academic Press).
- Luppi, P.H., Aston-Jones, G., Akaoka, H., Chouvet, G., and Jouviet, M. (1995). Afferent projections to the rat locus coeruleus demonstrated by retrograde and anterograde tracing with cholera-toxin B subunit and Phaseolus vulgaris leucoagglutinin. *Neuroscience* 65, 119–160.
- Martins, A.R.O., and Froemke, R.C. (2015). Coordinated forms of noradrenergic plasticity in the locus coeruleus and primary auditory cortex. *Nat. Neurosci.* 18, 1483–1492.
- Marzo, A., Totah, N.K., Neves, R.M., Logothetis, N.K., and Eschenko, O. (2014). Unilateral electrical stimulation of rat locus coeruleus elicits bilateral response of norepinephrine neurons and sustained activation of medial prefrontal cortex. *J. Neurophysiol.* 111, 2570–2588.
- McCormick, D.A., and Pape, H.C. (1990). Noradrenergic and serotonergic modulation of a hyperpolarization-activated cation current in thalamic relay neurones. *J. Physiol.* 431, 319–342.
- McCormick, D.A., and Prince, D.A. (1988). Noradrenergic modulation of firing pattern in guinea pig and cat thalamic neurons, *in vitro*. *J. Neurophysiol.* 59, 978–996.
- McCormick, D.A., McGinley, M.J., and Salkoff, D.B. (2015). Brain state dependent activity in the cortex and thalamus. *Curr. Opin. Neurobiol.* 31, 133–140.
- McGinley, M.J., David, S.V., and McCormick, D.A. (2015a). Cortical Membrane Potential Signature of Optimal States for Sensory Signal Detection. *Neuron* 87, 179–192.
- McGinley, M.J., Vinck, M., Reimer, J., Batista-Brito, R., Zagha, E., Cadwell, C.R., Tólias, A.S., Cardin, J.A., and McCormick, D.A. (2015b). Waking State: Rapid Variations Modulate Neural and Behavioral Responses. *Neuron* 87, 1143–1161.
- Moxon, K.A., Devilbiss, D.M., Chapin, J.K., and Waterhouse, B.D. (2007). Influence of norepinephrine on somatosensory neuronal responses in the rat thalamus: a combined modeling and *in vivo* multi-channel, multi-neuron recording study. *Brain Res.* 1147, 105–123.
- Murphy, P.R., O'Connell, R.G., O'Sullivan, M., Robertson, I.H., and Balsters, J.H. (2014). Pupil diameter covaries with BOLD activity in human locus coeruleus. *Hum. Brain Mapp.* 35, 4140–4154.
- Nassar, M.R., Rumsey, K.M., Wilson, R.C., Parikh, K., Heasley, B., and Gold, J.I. (2012). Rational regulation of learning dynamics by pupil-linked arousal systems. *Nat. Neurosci.* 15, 1040–1046.
- Ollerenshaw, D.R., Bari, B.A., Millard, D.C., Orr, L.E., Wang, Q., and Stanley, G.B. (2012). Detection of tactile inputs in the rat vibrissa pathway. *J. Neurophysiol.* 108, 479–490.
- Ollerenshaw, D.R., Zheng, H.J., Millard, D.C., Wang, Q., and Stanley, G.B. (2014). The adaptive trade-off between detection and discrimination in cortical representations and behavior. *Neuron* 81, 1152–1164.
- Otsu, N. (1979). A Threshold Selection Method from Gray-Level Histograms. *Systems, Man and Cybernetics. IEEE Transactions on* 9, 62–66.
- Payzan-LeNestour, E., Dunne, S., Bossaerts, P., and O'Doherty, J.P. (2013). The neural representation of unexpected uncertainty during value-based decision making. *Neuron* 79, 191–201.
- Picard, R.W., Fedor, S., and Ayzenberg, Y. (2016). Multiple Arousal Theory and Daily-Life Electrodermal Activity Asymmetry. *Emot. Rev.* 8, 62–75.
- Rajkowski, J., Majczynski, H., Clayton, E., and Aston-Jones, G. (2004). Activation of monkey locus coeruleus neurons varies with difficulty and performance in a target detection task. *J. Neurophysiol.* 92, 361–371.
- Ranck, J.B., Jr. (1975). Which elements are excited in electrical stimulation of mammalian central nervous system: a review. *Brain Res.* 98, 417–440.
- Reimer, J., Froudarakis, E., Cadwell, C.R., Yatsenko, D., Denfield, G.H., and Tólias, A.S. (2014). Pupil fluctuations track fast switching of cortical states during quiet wakefulness. *Neuron* 84, 355–362.
- Reimer, J., McGinley, M.J., Liu, Y., Rodenkirch, C., Wang, Q., McCormick, D.A., and Tólias, A.S. (2016). Pupil fluctuations track rapid changes in adrenergic and cholinergic activity in cortex. *Nat. Commun.* 7, 13289.
- Sara, S.J. (2009). The locus coeruleus and noradrenergic modulation of cognition. *Nat. Rev. Neurosci.* 10, 211–223.
- Sara, S.J., and Bouret, S. (2012). Orienting and reorienting: the locus coeruleus mediates cognition through arousal. *Neuron* 76, 130–141.
- Sara, S.J., Vankov, A., and Hervé, A. (1994). Locus coeruleus-evoked responses in behaving rats: a clue to the role of noradrenaline in memory. *Brain Res. Bull.* 35, 457–465.
- Savastano, L.E., Castro, A.E., Fitt, M.R., Rath, M.F., Romeo, H.E., and Muñoz, E.M. (2010). A standardized surgical technique for rat superior cervical ganglionectomy. *J. Neurosci. Methods* 192, 22–33.
- Simpson, K.L., Altman, D.W., Wang, L., Kirifides, M.L., Lin, R.C.S., and Waterhouse, B.D. (1997). Lateralization and functional organization of the locus coeruleus projection to the trigeminal somatosensory pathway in rat. *J. Comp. Neurol.* 385, 135–147.
- Steindler, D.A. (1981). Locus coeruleus neurons have axons that branch to the forebrain and cerebellum. *Brain Res.* 223, 367–373.
- Steinhauer, S.R., Siegle, G.J., Condray, R., and Pless, M. (2004). Sympathetic and parasympathetic innervation of pupillary dilation during sustained processing. *Int. J. Psychophysiol.* 52, 77–86.
- Steriade, M., McCormick, D.A., and Sejnowski, T.J. (1993). Thalamocortical oscillations in the sleeping and aroused brain. *Science* 262, 679–685.
- Szabadi, E. (2013). Functional neuroanatomy of the central noradrenergic system. *J. Psychopharmacol. (Oxford)* 27, 659–693.
- Thiebaut de Schotten, M., Dell'Acqua, F., Forkel, S.J., Simmons, A., Vergani, F., Murphy, D.G., and Catani, M. (2011). A lateralized brain network for visuo-spatial attention. *Nat. Neurosci.* 14, 1245–1246.
- Usher, M., Cohen, J.D., Servan-Schreiber, D., Rajkowski, J., and Aston-Jones, G. (1999). The role of locus coeruleus in the regulation of cognitive performance. *Science* 283, 549–554.
- Van Boven, R.W., Ingeholm, J.E., Beauchamp, M.S., Bikle, P.C., and Ungerleider, L.G. (2005). Tactile form and location processing in the human brain. *Proc. Natl. Acad. Sci. USA* 102, 12601–12605.
- Vazey, E.M., and Aston-Jones, G. (2014). Designer receptor manipulations reveal a role of the locus coeruleus noradrenergic system in isoflurane general anesthesia. *Proc. Natl. Acad. Sci. USA* 111, 3859–3864.
- Vinck, M., Batista-Brito, R., Knoblich, U., and Cardin, J.A. (2015). Arousal and locomotion make distinct contributions to cortical activity patterns and visual encoding. *Neuron* 86, 740–754.

- Wahn, B., Ferris, D.P., Hairston, W.D., and König, P. (2017). Pupil Size Asymmetries Are Modulated By An Interaction Between Attentional Load And Task Experience. *bioRxiv*. <http://dx.doi.org/10.1101/137893>.
- Wang, Q., Webber, R.M., and Stanley, G.B. (2010). Thalamic synchrony and the adaptive gating of information flow to cortex. *Nat. Neurosci.* **13**, 1534–1541.
- Wang, Q., Millard, D.C., Zheng, H.J.V., and Stanley, G.B. (2012). Voltage-sensitive dye imaging reveals improved topographic activation of cortex in response to manipulation of thalamic microstimulation parameters. *J. Neural Eng.* **9**, 026008.
- Wekselblatt, J.B., and Niell, C.M. (2015). Behavioral State–Getting “In The Zone”. *Neuron* **87**, 7–9.
- Zheng, H.J.V., Wang, Q., and Stanley, G.B. (2015). Adaptive shaping of cortical response selectivity in the vibrissa pathway. *J. Neurophysiol.* **113**, 3850–3865.